Available online on 15.02.2019 at http://jddtonline.info

Journal of Drug Delivery and Therapeutics

Open Access to Pharmaceutical and Medical Research

Open Access Research Article

Structural and quantum chemical studies on aryl sulfonyl piperazine derivatives

Tahar Abbaz[1*], Amel Bendjeddou[1] and Didier Villemin[2]

[1] Laboratory of Aquatic and Terrestrial Ecosystems, Org. and Bioorg. Chem. Group, University of Mohamed-Cherif Messaadia, Souk Ahras, 41000, Algeria

[2] Laboratory of Molecular and Thio-Organic Chemistry, UMR CNRS 6507, INC3M, FR 3038, Labex EMC3, ensicaen & University of Caen, Caen 14050, France

ABSTRACT

The optimized molecular structure and electronic features of aryl sulfonyl piperazine derivatives **1-4** have been investigated theoretically using Gaussian 09 software package and DFT/B3LYP method with 6-31G (d,p) basis set. The reactivity of the title molecules was investigated and both the positive and negative centers of the molecules were identified using molecular electrostatic potential (MEP) analysis which the results illustrate that the regions reveal the negative electrostatic potential are localized in sulfamide function while the regions presenting the positive potential are localized in the hydrogen atoms. The energies of the frontier molecular orbitals and LUMO-HOMO energy gap are measured to explain the electronic transitions. Global reactivity parameters of the aryl sulfonyl piperazine derivatives molecules were predicted to find that the more reactive and softest compound is the compound **3**. Mulliken's net charges have been calculated and results show that 3N is the more negative and 33S is the more positive charge, which Indicates extensive charge delocalization in the entire molecule. The stability of the molecule arising from hyper-conjugative interaction and charge delocalization (π→π transitions) has been analyzed using NBO analysis. Fist hyperpolarizability is calculated in order to find its importance in non-linear optics and the results show that the studied molecules have not the NLO applications.

Keywords: sulfamide; density functional theory; computational chemistry; electronic structure; quantum chemical calculations.

Article Info: Received 19 Dec 2018; Review Completed 23 Jan 2019; Accepted 26 Jan 2019; Available online 15 Feb 2019

Cite this article as:

Abbaz T, Bendjeddou A, Villemin D, Structural and quantum chemical studies on aryl sulfonyl piperazine derivatives, Journal of Drug Delivery and Therapeutics. 2019; 9(1-s):88-97 **DOI: http://dx.doi.org/10.22270/jddt.v9i1-s.2264**

***Address for Correspondence:**

Tahar Abbaz, Laboratory of Aquatic and Terrestrial Ecosystems, Org. and Bioorg. Chem. Group, University of Mohamed-Cherif Messaadia, Souk Ahras, 41000, Algeria

1. INTRODUCTION

Sulfonamides, called sulfa drugs, a derivative or variation of sulfanilamide, act as antimicrobial agents by inhibiting bacterial growth and activity[1]. Also Sulfonamides were the first synthetic antibiotics to be used in clinic and they exhibit interesting pharmacological properties, such as selectivity to bacterial cells and low toxicity. Later on, a large number of sulfonamides derivatives were synthesized, characterized and tested for antibacterial[2], antitumor[3], anti-carbonic anhydrase[4,5], diuretic[6,7], hypoglycaemic[8], antithyroid[9] or protease inhibitory activity[10,11] among others.

Conceptual density functional theory has been successfully exploited to understand the chemical reactivity and site selectivity of a variety of molecular systems[12]. DFT offers a better compromise between computational cost and accuracy for medium size molecules, and hence it has been successfully applied in many previous studies[13].

In this paper, we report a quantum chemical investigation of aryl sulfonyl piperazine derivatives **1-4** reported in literature[14] at DFT/B3LYP method and 6-31G (d,p) basis set. The optimized geometrical parameters are computed by same method. Various properties like Molecular Electrostatic Potential (MEP) analysis, Highest Occupied Molecular Orbital (HOMO), Lowest Unoccupied Molecular Orbital (LUMO) energies, and Natural Bond Orbital (NBO) of the aryl sulfonyl piperazine derivatives molecules are performed to elucidate the information regarding charge transfer within the molecule. The molecular quantities as affinity (A), ionization potential (I), electronic chemical potential (μ), global hardness (η), global softness (S), electronegativity (χ), electrophilicity indices (ω) are calculated and discussed. Also, Mulliken charges are investigated to explain the chemical selectivity or reactivity site in studied molecules. Non-linear optical properties of the molecules are predicted in order to gain deeper knowledge about the relationship between molecular architecture, non-linear response, and the hyperpolarizability and support the efforts towards

discovery of new efficient products for therapeutic applications.

2. MATERIALS AND METHODS

In this study, all calculations were carried out with the Gauss-View[15] molecular visualization program and Gaussian 09W[16] package program on personal computer. The optimized molecular structure and quantum chemical calculus of the title compounds have been calculated by using B3LYP (Becke's three-parameter hybrid model using the Lee-Yang Parr correlation functional)[17] method with 6-31G (d,p) basis set.

3. RESULTS AND DISCUSSION

3.1. Molecular Geometry:

The optimized structure parameters of aryl sulfonyl piperazine derivatives **1-4** is calculated by DFT level with B3LYP/6-31G (d,p) basis set shown in Tables 1-4 in accordance with the atom numbering scheme given in Figure 1.

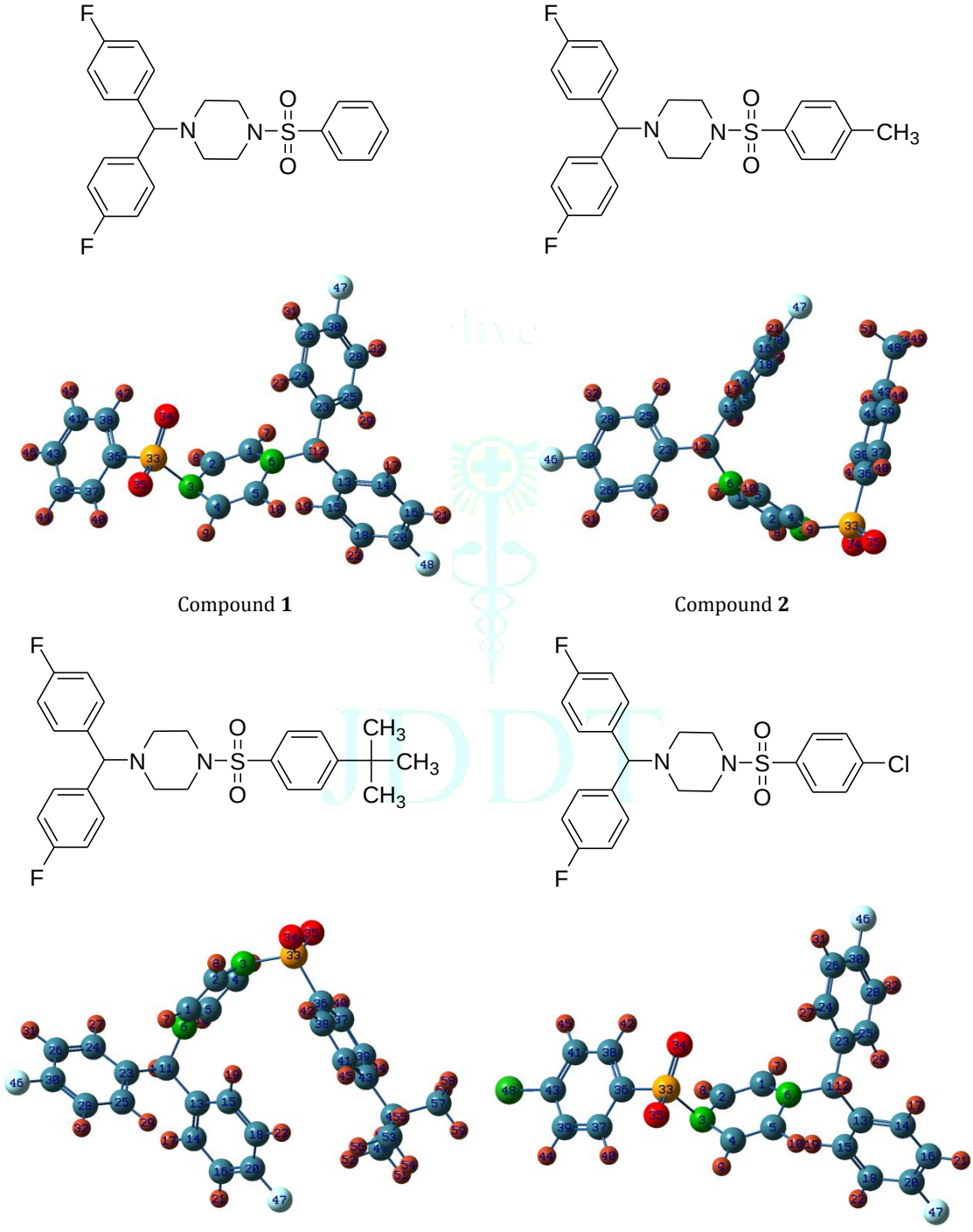

Compound **1** Compound **2**

Compound **3** Compound **4**

Figure 1: Optimized molecular structure of aryl sulfonyl piperazine derivatives **1-4**

Table 1: Optimized geometric parameters of compound **1**

Bond Length (Å)		Bond Angles (°)		Dihedral Angles (°)	
R(1,2)	1.343	A(2,1,6)	121.536	D(2,1,6,11)	174.105
R(1,7)	1.083	A(6,1,7)	116.603	D(1,2,3,33)	104.325
R(2,3)	1.437	A(1,2,8)	121.618	D(8,2,3,4)	156.621
R(2,8)	1.083	A(3,2,8)	116.670	D(9,4,5,6)	175.906
R(3,33)	1.776	A(4,3,33)	111.450	D(10,5,6,1)	159.357
R(4,9)	1.081	A(3,4,5)	121.206	D(12,11,13,15)	140.747
R(5,6)	1.398	A(4,5,6)	121.971	D(17,14,16,20)	179.878
R(6,11)	1.472	A(1,6,11)	122.161	D(21,16,20,18)	179.375
R(11,23)	1.532	A(16,14,17)	119.153	D(15,18,20,48)	179.858
R(14,16)	1.393	A(18,15,19)	119.010	D(11,23,24,26)	179.561
R(15,18)	1.396	A(14,16,20)	118.505	D(25,28,30,47)	179.901
R(16,20)	1.391	A(20,16,21)	119.718	D(32,28,30,26)	179.868
R(23,25)	1.398	A(15,18,22)	121.521	D(3,33,36,37)	72.457
R(24,26)	1.391	A(11,23,24)	118.400	D(40,37,39,43)	179.279
R(25,28)	1.397	A(30,26,31)	119.739	D(36,38,41,45)	179.796

Table 2: Optimized geometric parameters of compound **2**

Bond Length (Å)		Bond Angles (°)		Dihedral Angles (°)	
R(1,6)	1.408	A(2,1,7)	120.715	D(6,1,2,8)	171.781
R(1,7)	1.083	A(6,1,7)	115.814	D(2,1,6,11)	152.316
R(2,3)	1.429	A(1,2,3)	121.852	D(7,1,6,5)	171.385
R(3,33)	1.725	A(2,3,4)	114.822	D(2,3,4,9)	169.039
R(4,9)	1.081	A(4,5,6)	123.291	D(33,3,4,5)	138.339
R(5,6)	1.406	A(6,5,10)	115.685	D(3,4,5,10)	175.669
R(6,11)	1.476	A(1,6,5)	115.117	D(5,6,11,13)	79.246
R(11,23)	1.534	A(14,13,15)	118.392	D(13,11,23,24)	167.499
R(13,14)	1.400	A(16,14,17)	118.988	D(19,15,18,20)	179.828
R(15,18)	1.393	A(13,15,19)	119.965	D(15,18,20,47)	179.532
R(16,21)	1.084	A(18,15,19)	118.946	D(22,18,20,16)	179.929
R(20,47)	1.355	A(14,16,20)	118.305	D(23,24,26,31)	179.652
R(23,24)	1.404	A(11,23,25)	121.969	D(27,24,26,30)	179.921
R(25,28)	1.396	A(24,23,25)	118.387	D(24,26,30,46)	179.938
R(30,46)	1.349	A(30,26,31)	119.691	D(3,33,36,37)	87.622

Table 3: Optimized geometric parameters of compound **3**

Bond Length (Å)		Bond Angles (°)		Dihedral Angles (°)	
R(1,2)	1.340	A(2,1,6)	122.709	D(6,1,2,8)	172.016
R(1,6)	1.404	A(6,1,7)	115.981	D(7,1,6,5)	170.211
R(2,3)	1.432	A(1,2,8)	122.420	D(2,3,4,9)	167.050
R(2,8)	1.081	A(3,2,8)	115.614	D(33,3,4,5)	136.493
R(3,4)	1.431	A(2,3,33)	117.732	D(1,6,11,12)	160.356
R(4,9)	1.081	A(5,4,9)	122.550	D(12,11,13,15)	149.760
R(5,6)	1.404	A(4,5,10)	120.900	D(17,14,16,20)	179.815
R(6,11)	1.470	A(1,6,5)	115.719	D(13,15,18,22)	179.336
R(13,14)	1.401	A(6,11,13)	113.745	D(21,16,20,18)	179.440
R(15,18)	1.394	A(16,14,17)	119.115	D(11,23,24,26)	179.584
R(16,20)	1.390	A(13,15,18)	120.926	D(25,23,24,27)	179.341
R(20,47)	1.353	A(20,16,21)	119.801	D(24,23,25,29)	179.691
R(24,26)	1.391	A(23,25,28)	120.970	D(23,25,28,32)	179.966
R(25,28)	1.397	A(24,26,31)	121.782	D(31,26,30,28)	179.917
R(30,46)	1.348	A(30,26,31)	119.682	D(40,37,39,43)	177.472

Table 4: Optimized geometric parameters of compound **4**

Bond Length (Å)		Bond Angles (°)		Dihedral Angles (°)	
R(1,2)	1.343	A(2,1,7)	121.556	D(2,1,6,11)	171.982
R(1,6)	1.394	A(6,1,7)	116.621	D(1,2,3,33)	106.006
R(2,8)	1.083	A(1,2,3)	121.854	D(8,2,3,4)	157.757
R(3,33)	1.775	A(3,2,8)	116.629	D(33,3,4,9)	72.511
R(4,9)	1.081	A(2,3,33)	113.624	D(9,4,5,6)	176.194
R(5,10)	1.084	A(4,3,33)	111.660	D(1,6,11,12)	157.339
R(6,11)	1.474	A(4,5,10)	121.424	D(23,11,13,14)	78.378
R(11,12)	1.097	A(1,6,11)	122.008	D(12,11,23,25)	129.137
R(11,23)	1.531	A(5,6,11)	118.716	D(14,13,15,19)	178.600
R(13,15)	1.400	A(12,11,23)	106.146	D(13,15,18,22)	179.677
R(14,16)	1.393	A(13,11,23)	114.499	D(15,18,20,47)	179.858
R(15,18)	1.396	A(11,13,14)	118.933	D(11,23,24,26)	179.641
R(16,20)	1.391	A(15,18,22)	121.516	D(25,23,24,27)	178.856
R(20,47)	1.349	A(20,18,22)	119.644	D(23,25,28,32)	179.878
R(23,24)	1.404	A(26,24,27)	119.383	D(3,33,36,37)	70.199

3.2. Molecular Electrostatic Potential (MEP):

Molecular electrostatic potential and electrostatic potential are useful quantities to illustrate the charge distributions of molecules and used to visualize variably charged regions of a molecule. Therefore, the charge distributions can predict how the molecules interact with another molecule. To predict reactive sites for electrophilic and nucleophilic attack for the investigated molecules, the MEP at the B3LYP/6-31G (d,p) optimized geometries were calculated and presented in Figure 2 . The different values of the electrostatic potential at the surface are represented by different colors with the Potential increases in the order red < orange < yellow < green < blue.

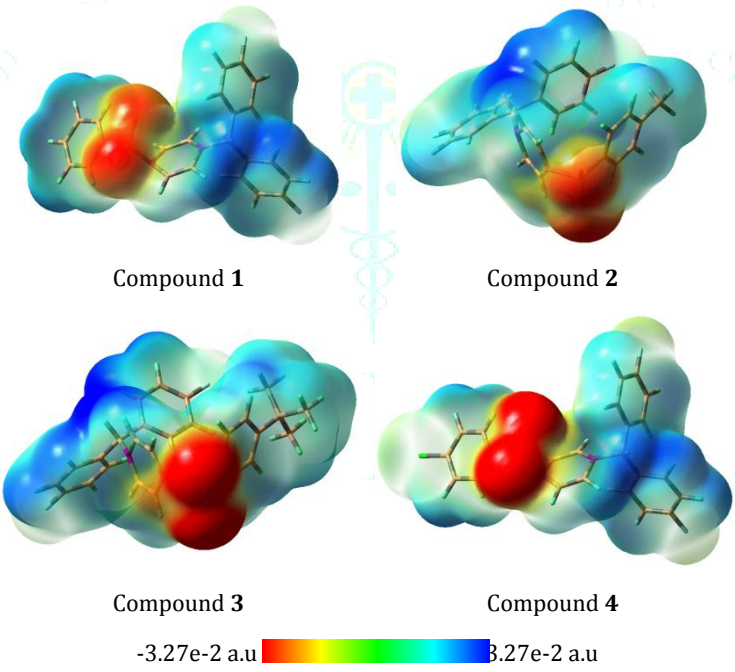

Figure 2: Molecular electrostatic potential surface of aryl sulfonyl piperazine derivatives **1-4**

In all molecules, the regions exhibiting the negative electrostatic potential are localized on sulfamide function; while the regions presenting the positive potential are localized vicinity of the hydrogen atoms.

3.3. Basin analysis

The concept of basin was first introduced by Bader in his atom in molecular (AIM) theory, after that, this concept was transplant to the analysis of ELF by Savin and Silvi. In fact, basin can be defined for any real space function, such as molecular orbital, electron density difference, electrostatic potential and even Fukui function.

A real space function in general has one or more maxima, which are referred to as attractors or (3,-3) critical points. Each basin is a subspace of the whole space, and uniquely contains an attractor. The basins are separated with each other by interbasin surfaces (IBS), which are essentially the zero-flux surface of the real space functions; mathematically, such surfaces consist of all of the points **r** satisfying $\nabla f(\mathrm{r}).\mathrm{n}(\mathrm{r}) = 0$, where n(r) stands for the unit normal vector of the surface at position r.

Interbasin surfaces (IBS) dissect the whole molecular space into individual basins, each IBS actually is a bunch of gradient paths derived from a (3,-1) critical points (CP). The interbasin surfaces of compounds **1-4** generated by (3,-1) critical points are illustrated below.

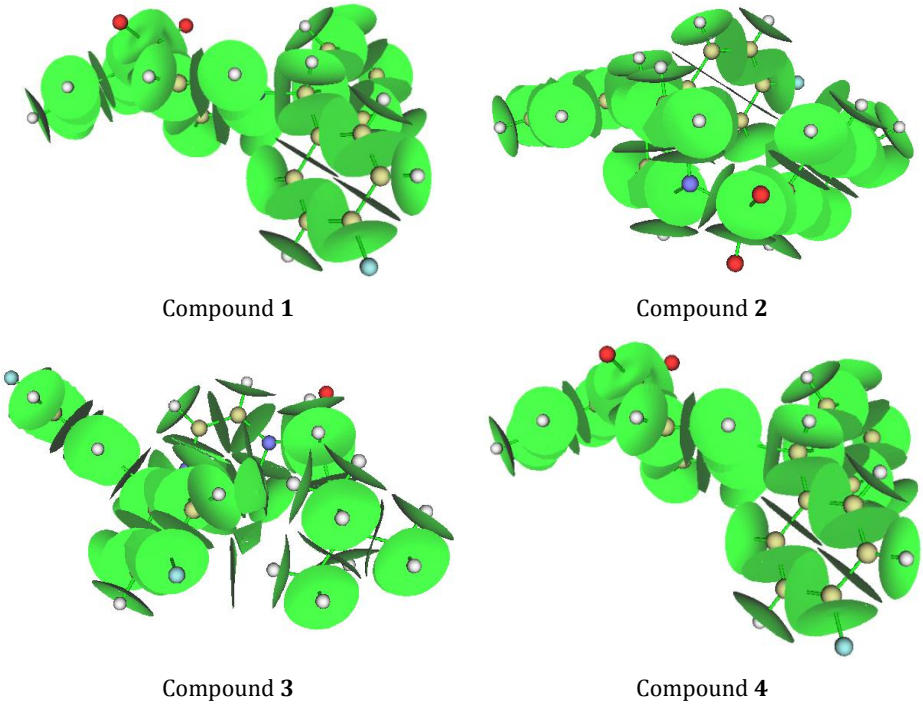

Figure 3: Plots of the interbasin surfaces of compounds **1-4**
*The number of interbasin surfaces is 51, 57, 69 and 51 for compounds **1-4** respectively.*

3.4. Frontier Molecular Orbitals (FMOs):

The HOMO energy designates the electron donating ability while the LUMO designates the electron accepting ability and the gap between HOMO-LUMO characterizes the molecular chemical stability[18,19]. A molecule with a small frontier orbital gap is highly polarizable and is generally associated with a high chemical reactivity. The HOMO and LUMO orbitals of compound **3** with a small energy gap were computed by the DFT/B3LYP method with 6-31G (d,p) basis set and visualized in Figure 4.

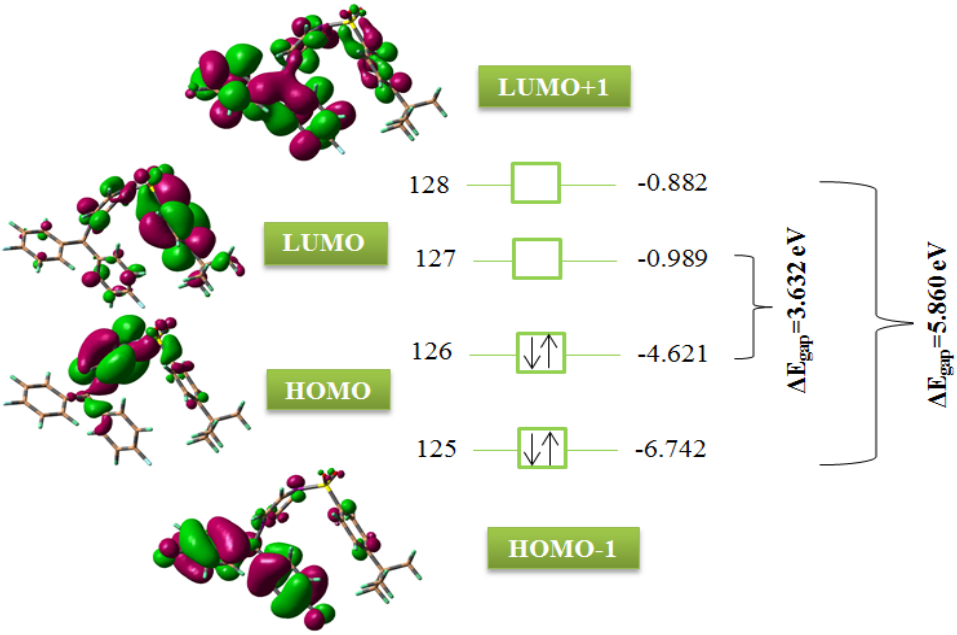

Figure 4: HOMO-LUMO Structure with the energy level diagram of compound **3**

HOMO-1 and LUMO+1 are confined over the bis(4-fluor-ophenyl)-methyl, while HOMO and LUMO are on piperazine and sulfamide function for compound **3** which gives charge transfer process in the molecular system.

3.5. Global Reactivity Descriptors:

The understanding of chemical reactivity and site selectivity of the molecular systems have been effectively handled by the conceptual density functional theory (DFT)[20]. Chemical potential, global hardness, global softness, electronegativity and electrophilicity are global reactivity descriptors, highly successful in predicting global chemical reactivity trends. The global parameters such as ionization potential (I), electron affinity (A), electrophilicity (ω), electronegativity (χ), hardness (η), and softness (S) of the title molecules are determined by the DFT/B3LYP method with 6-31G (d,p) basis set and displayed in Table 5.

Table 5: Quantum chemical descriptors of aryl sulfonyl piperazine derivatives **1-4**

Parameters	Compound 1	Compound 2	Compound 3	Compound 4
EHOMO (eV)	-4.869	-4.668	-4.621	-4.969
ELUMO (eV)	-1.016	-0.936	-0.989	-1.281
ΔEgap (eV)	3.854	3.733	3.632	3.688
I (eV)	4.869	4.668	4.621	4.969
A (eV)	1.016	0.936	0.989	1.281
μ (eV)	-2.943	-2.802	-2.805	-3.125
χ (eV)	2.943	2.802	2.805	3.125
η (eV)	1.927	1.866	1.816	1.844
S (eV)	0.259	0.268	0.275	0.271
ω (eV)	2.247	2.103	2.167	2.648

The compound which has the lowest energy gap is the compound **3** (ΔE_{gap} = 3.632 eV). This lower gap allows it to be the softest molecule. The compound that has the highest energy gap is the compound **1** (ΔE_{gap} = 3.854 eV). The compound that has the highest HOMO energy is the compound **3** (E_{HOMO} = -4.621 eV). This higher energy allows it to be the best electron donor. The compound that has the lowest LUMO energy is the compound **4** (E_{LUMO} = -1.281 eV) which signifies that it can be the best electron acceptor. The two properties like *I* (potential ionization) and *A* (affinity) are so important, the determination of these two properties allows us to calculate the absolute electronegativity (χ) and the absolute hardness (η). These two parameters are related to the one-electron orbital energies of the HOMO and LUMO respectively. Compound **3** has the lowest value of the potential ionization (*I* = 4.621 eV), so that will be the better electron donor. Compound **4** has the largest value of the affinity (*A* = 1.281 eV), so it is the better electron acceptor. The chemical reactivity varies with the structure of molecules. Chemical hardness (softness) value of compound **3** (η = 1.816 eV, **S** = 0.275 eV) is lesser (greater) among all the molecules. Thus, compound **3** is found to be more reactive than all the compounds. Compound **4** possesses higher electronegativity value (χ = 3.125 eV) than all compounds so; it is the best electron acceptor. The value of ω for compound **4** (ω = 2.648 eV) indicates that it is the stronger electrophiles than all compounds. Compound **3** has the smaller frontier orbital gap so, it is more polarizable and is associated with a high chemical reactivity, low kinetic stability and is also termed as soft molecule.

3.6. Mulliken analysis:

The atomic charge in molecules is fundamental parameter in the chemistry study. For instance, atomic charge has been used to describe the processes of electronegativity equalization and charge transfer in chemical reactions[21], and to model the electrostatic potential outside molecular surfaces[22]. Mulliken atomic charges calculated at the DFT/B3LYP levels with 6-31G (d,p) basis set of compound **3** which is the more reactive and are detailed in a Mulliken's plot as visualized in Figure 5.

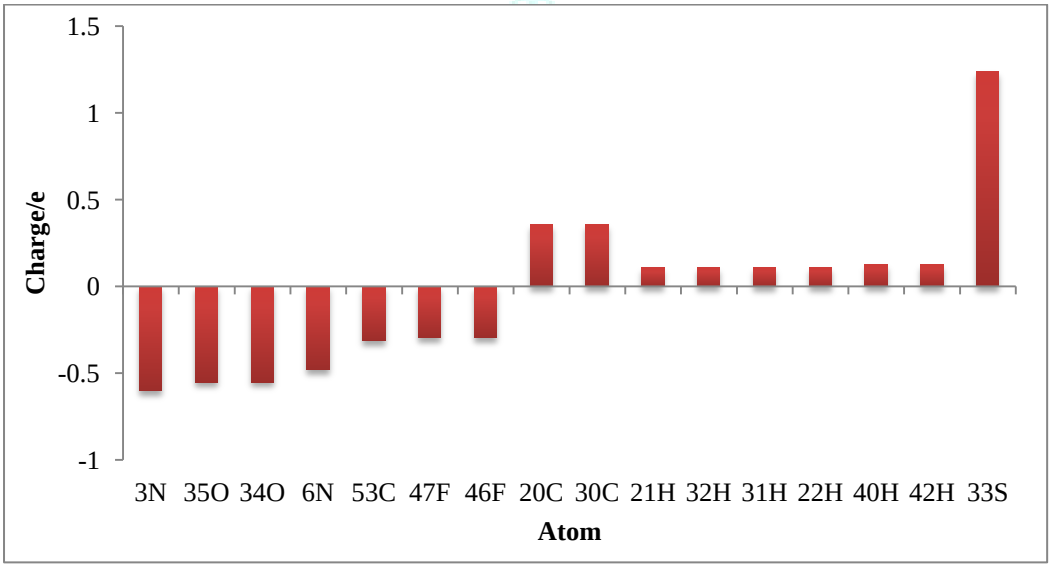

Figure 5: Mulliken's plot of compound **3**

The atom 3N shows more negative (-0.602615e) charge and 33S more positive (1.234402e) charge, which suggests extensive charge delocalization in the entire molecule. The charge noticed on the 6N and 3N is smaller in piperazine and equal to -0.479801e and -0.602615e respectively. This can be explained by the high degree of conjugation, with a strong push-pull effect between the sulfamide group, piperazine and bis(4-fluor-ophenyl)-methyl. Negatively charged oxygen (35O, 34O) atoms shows that charge is transferred from sulfur to oxygen. Carbon atom 53C is more negatively charged which indicate that the charge transfer from sulfamide group to tert-butyl group through benzene ring. The negative charge of 47F and 46F is equal to -0.297266e and -0.293365e respectively, which explain that, is due to the most positive charge of carbons attached to fluorine atoms. The maximum atomic charge of carbons is obtained for 20C and 30C. This is due to the attachment of negatively charged fluorine. The positive charges are localized on the hydrogen

atoms. Very similar values of positive charges are observed for the hydrogen atoms bonded to the carbon atoms in benzene rings (21H, 32H, 31H, 22H, 40H and 42H (0.10~0.12e)).

3.7. Natural Bond Orbital Analysis (NBO):

The NBO method demonstrates the bonding concepts like atomic charge, Lewis structure, bond type, hybridization, bond order, charge transfer and resonance possibility. Natural bond orbital (NBO) analysis is a very useful tool for understanding delocalization of electron density from occupied Lewis-type (donor) NBOs to properly unoccupied non-Lewis type (acceptor) NBOs within the molecule. The stabilization of orbital interaction is proportional to the energy difference between interacting orbitals. Therefore, the interaction having the strongest stabilization takes place between effective donors and effective acceptors. The stabilization energy E (2) values of the aryl sulfonyl piperazine derivatives **1-4** were calculated on the basis of second-order Fock matrix perturbation theory using B3LYP/6-31G (d,p) basis set. The larger E (2) values were listed in Tables 6-9.

Table 6: Second order perturbation theory analysis of Fock matrix on NBO of compound **1**

Donor(i)	ED/e	Acceptor(j)	ED/e	E(2) Kcal/mol	E(j)-E(i) a.u	F(i.j) a.u
LP (1) N6	1.68745	π*(C1-C2)	0.17895	32.52	0.30	0.092
LP (1) N6	1.68745	π*(C4-C5)	0.16538	30.23	0.31	0.090
LP (3) O34	1.77159	σ*(N3-S33)	0.34969	26.35	0.35	0.088
π (C41-C43)	1.65399	π*(C36-C38)	0.37181	23.38	0.27	0.071
π (C24-C26)	1.68584	π*(C28-C30)	0.36491	23.00	0.28	0.072
LP (3) O35	1.79229	σ*(N3-S33)	0.34969	22.62	0.35	0.082
π (C14-C16)	1.68992	π*(C18-C20)	0.36921	22.29	0.28	0.072
π (C13-C15)	1.66693	π*(C14-C16)	0.33525	21.55	0.28	0.069
π (C37-C39)	1.65119	π*(C41-C43)	0.31429	21.15	0.28	0.069
π (C23-C25)	1.67927	π*(C24-C26)	0.31527	21.10	0.29	0.069
π (C28-C30)	1.66331	π*(C23-C25)	0.35486	21.05	0.30	0.071
π (C18-C20)	1.65778	π*(C13-C15)	0.35319	20.78	0.30	0.070
LP (3) F47	1.91557	π*(C28-C30)	0.36491	20.58	0.42	0.090
π (C36-C38)	1.68683	π*(C37-C39)	0.29769	20.45	0.30	0.070
LP (3) F48	1.91630	π*(C18-C20)	0.36921	20.38	0.42	0.089
π (C37-C39)	1.65119	π*(C36-C38)	0.37181	19.15	0.27	0.065
LP (2) O35	1.80006	σ*(S33-C36)	0.20128	19.09	0.44	0.082
π (C13-C15)	1.66693	π*(C18-C20)	0.36921	19.03	0.28	0.065
π (C18-C20)	1.65778	π*(C14-C16)	0.33525	18.97	0.29	0.067
LP (2) O34	1.80759	σ*(S33-C36)	0.20128	18.71	0.45	0.082

Table 7: Second order perturbation theory analysis of Fock matrix on NBO of compound **2**

Donor(i)	ED/e	Acceptor(j)	ED/e	E(2) Kcal/mol	E(j)-E(i) a.u	F(i.j) a.u
π (C41-C43)	1.62764	π*(C36-C38)	0.39916	25.84	0.26	0.074
π (C15-C18)	1.68532	π*(C16-C20)	0.37059	22.71	0.28	0.072
π (C24-C26)	1.68675	π*(C28-C30)	0.36894	22.71	0.28	0.072
π (C37-C39)	1.66158	π*(C41-C43)	0.33344	22.01	0.29	0.071
π (C23-C25)	1.66996	π*(C24-C26)	0.32878	21.54	0.28	0.070
π (C36-C38)	1.68205	π*(C37-C39)	0.30414	21.20	0.29	0.071
π (C13-C14)	1.66806	π*(C15-C18)	0.32785	21.14	0.28	0.069
π (C28-C30)	1.65834	π*(C23-C25)	0.35560	21.13	0.30	0.071
LP (3) F46	1.91591	π*(C28-C30)	0.36894	20.47	0.42	0.090
π (C16-C20)	1.66376	π*(C13-C14)	0.35317	20.42	0.30	0.070
LP (3) F47	1.91691	π*(C16-C20)	0.37059	19.35	0.43	0.088
π (C13-C14)	1.66806	π*(C16-C20)	0.37059	19.18	0.27	0.065
LP (3) O35	1.77649	σ*(S33-O34)	0.14724	18.73	0.57	0.094
π (C16-C20)	1.66376	π*(C15-C18)	0.32785	18.69	0.30	0.067
π (C23-C25)	1.66996	π*(C28-C30)	0.36894	18.68	0.28	0.065
LP (1) N6	1.73127	π*(C1-C2)	0.14791	18.66	0.35	0.075
π (C28-C30)	1.65834	π*(C24-C26)	0.32878	18.61	0.29	0.066
LP (3) O34	1.77726	σ*(S33-O35)	0.14753	18.61	0.57	0.094
LP (1) N6	1.73127	π*(C4-C5)	0.14728	18.37	0.36	0.075
π (C15-C18)	1.68532	π*(C13-C14)	0.35317	18.28	0.29	0.065

Table 8: Second order perturbation theory analysis of Fock matrix on NBO of compound **3**

Donor(i)	ED/e	Acceptor(j)	ED/e	E(2) Kcal/mol	E(j)-E(i) a.u	F(i.j) a.u
π (C41-C43)	1.63850	π*(C36-C38)	0.38934	25.16	0.27	0.073
π (C24-C26)	1.69009	π*(C28-C30)	0.36464	22.63	0.28	0.072
π (C14-C16)	1.68625	π*(C18-C20)	0.37281	22.41	0.28	0.072
LP (1) N6	1.71819	π*(C1-C2)	0.15766	22.22	0.34	0.080
π (C13-C15)	1.65802	π*(C14-C16)	0.34164	22.08	0.28	0.070
LP (1) N6	1.71819	π*(C4-C5)	0.15104	21.57	0.34	0.079
π (C23-C25)	1.67382	π*(C24-C26)	0.32263	21.47	0.28	0.069
π (C37-C39)	1.66601	π*(C41-C43)	0.32543	21.12	0.29	0.070
π (C28-C30)	1.66139	π*(C23-C25)	0.35152	21.04	0.30	0.071
π (C36-C38)	1.68721	π*(C37-C39)	0.29460	20.72	0.30	0.070
π (C18-C20)	1.65590	π*(C13-C15)	0.35381	20.67	0.30	0.070
LP (3) F46	1.91534	π*(C28-C30)	0.36464	20.60	0.42	0.090
LP (3) F47	1.91800	π*(C18-C20)	0.37281	19.62	0.43	0.088
π (C13-C15)	1.65802	π*(C18-C20)	0.37281	19.57	0.27	0.066
π (C18-C20)	1.65590	π*(C14-C16)	0.34164	19.25	0.29	0.067
LP (3) O35	1.77509	σ*(S33-O34)	0.14735	19.11	0.57	0.095
LP (3) O34	1.77755	σ*(S33-O35)	0.14831	19.04	0.57	0.095
π (C14-C16)	1.68625	π*(C13-C15)	0.35381	18.55	0.29	0.066
π (C23-C25)	1.67382	π*(C28-C30)	0.36464	18.40	0.28	0.064
π (C28-C30)	1.66139	π*(C24-C26)	0.32263	18.31	0.29	0.066

Table 9: Second order perturbation theory analysis of Fock matrix on NBO of compound **4**

Donor(i)	ED/e	Acceptor(j)	ED/e	E(2) Kcal/mol	E(j)-E(i) a.u	F(i.j) a.u
LP (1) N6	1.68809	π*(C1-C2)	0.17926	32.66	0.31	0.092
LP (1) N6	1.68809	π*(C4-C5)	0.16536	30.27	0.31	0.090
LP (3) O34	1.77062	σ*(N3-S33)	0.35040	26.30	0.35	0.088
π (C24-C26)	1.68605	π*(C28-C30)	0.36452	22.94	0.28	0.072
π (C14-C16)	1.68963	π*(C18-C20)	0.36884	22.30	0.28	0.072
π (C37-C39)	1.65605	π*(C41-C43)	0.37555	22.11	0.27	0.069
π (C13-C15)	1.66765	π*(C14-C16)	0.33461	21.52	0.28	0.069
π (C41-C43)	1.66999	π*(C36-C38)	0.37103	21.34	0.29	0.071
π (C23-C25)	1.67859	π*(C24-C26)	0.31617	21.17	0.28	0.069
LP (3) O35	1.79152	σ*(N3-S33)	0.35040	21.17	0.35	0.080
π (C28-C30)	1.66197	π*(C23-C25)	0.35547	21.12	0.30	0.071
π (C36-C38)	1.68326	π*(C37-C39)	0.29191	20.98	0.29	0.071
π (C18-C20)	1.65728	π*(C13-C15)	0.35415	20.82	0.30	0.070
LP (3) F46	1.91524	π*(C28-C30)	0.36452	20.63	0.42	0.090
LP (3) F47	1.91608	π*(C18-C20)	0.36884	20.42	0.42	0.089
LP (2) O35	1.79866	σ*(S33-C36)	0.20305	19.42	0.44	0.083
π (C13-C15)	1.66765	π*(C18-C20)	0.36884	18.98	0.28	0.065
π (C18-C20)	1.65728	π*(C14-C16)	0.33461	18.95	0.29	0.067
LP (2) O34	1.80641	σ*(S33-C36)	0.20305	18.94	0.45	0.082
π (C14-C16)	1.68963	π*(C13-C15)	0.35415	18.42	0.29	0.066

The intra molecular interaction for the title compounds is formed by the orbital overlap between: π (C41-C43) and π*(C36-C38) for compound **1**, π (C41-C43) and π*(C36-C38) for compound **2**, π (C41-C43) and π*(C36-C38) for compound **3** and π (C24-C26) and π*(C28-C30) for compound **4** respectively, which result into intermolecular charge transfer (ICT) causing stabilization of the system. The intra molecular hyper conjugative interactions of π (C41-C43) to π*(C36-C38) for compound **1**, π (C41-C43) to π*(C36-C38) for compound **2**, π (C41-C43) to π*(C36-C38) for compound **3** and π (C24-C26) to π*(C28-C30) for compound **4** lead to highest stabilization of 23.38, 25.84, 25.16 and 22.94 kJ mol^{-1} respectively. In case of LP (1) N6 orbital to the π*(C1-C2) for compound **1**, LP (3) F46 orbital to π*(C36-C38) for compound **2**, LP (1) N6 orbital to π*(C1-C2) for compound **3**, LP (1) N6 orbital to π*(C1-C2) for compound **4** respectively, show the stabilization energy of 32.52, 20.47, 22.22 and 32.66 kJ mol^{-1} respectively.

3.8. Nonlinear Optical Properties (NLO):

Quantum chemical methods are presently used[23] for predicting the molecular NLO properties of different molecules. Hyperpolarizability is useful for understand the relationship between the molecular structure and nonlinear optical properties. The dipole moment (μ), polarizability (α), anisotropy of polarizability (Δα) and first hypepolarizability (β_0) of aryl sulfonyl piperazine derivatives **1-4** were calculated using B3LYP/6-31G (d,p) basis set and illustrated in Table 10.

Table 10: The dipole moments μ, polarizability α, the anisotropy of the polarizability Δα and the first hyperpolarizability β_0 of aryl sulfonyl piperazine derivatives **1-4**

Parameters	Compound 1	Compound 2	Compound 3	Compound 4
β_{xxx}	-80.1418	33.8770	71.1930	72.8004
β_{yyy}	-18.0889	56.9757	-135.5977	-12.5066
β_{zzz}	-19.4441	6.2440	-7.3554	-36.2879
β_{xyy}	-56.5413	-80.1818	-80.4397	-73.7287
β_{xxy}	13.3854	83.8699	-22.5999	7.4925
β_{xxz}	-81.4674	17.4466	-35.9068	23.1634
β_{xzz}	34.2293	3.1743	-11.4828	63.7969
β_{yzz}	8.5284	22.2646	-14.7475	8.0091
β_{yyz}	9.6757	5.1944	-7.3493	14.6975
β_{xyz}	-10.5785	-1.3550	-6.2189	-4.5413
β_0(esu)x10^{-33}	140.3301	171.1710	181.3870	62.9596
μ_x	1.2906	-2.8244	-1.4657	2.7242
μ_y	-0.5497	5.4337	-5.8459	-0.7656
μ_z	-3.1394	1.4130	-1.5114	-2.1005
μ(D)	3.4386	6.2848	6.2135	3.5241
α_{xx}	-164.4983	-199.7583	-198.5984	-187.7840
α_{yy}	-181.5728	-198.3003	-233.0360	-191.8492
α_{zz}	-175.4662	-171.1366	-192.6896	-195.2071
α_{xy}	1.9229	21.4815	-15.7292	2.0244
α_{xz}	24.6749	-1.4383	7.5540	13.1841
α_{yz}	-0.9038	-2.4431	-2.5963	-2.0240
α(esu)x10^{-24}	45.4385	46.7769	48.5591	24.2384
$\Delta\alpha$(esu)x10^{-24}	6.7340	6.9323	7.1965	3.5921

Since the values of the polarizabilities (Δα) and the hyperpolarizabilities (β_0) of the GAUSSIAN 09 output are obtained in atomic units (a.u.), the calculated values have been converted into electrostatic units (e.s.u.) (for α; 1 a.u = 0.1482 x 10^{-24} e.s.u., for β; 1 a.u = 8.6393 x 10^{-33} e.s.u.). The calculated values of dipole moment (μ) for the title compounds were found to be 3.4386, 6.2848, 6.2135 and 3.5241 D respectively, which are approximately three and six times than to the value for urea (μ = 1.3732 D). Urea is one of the prototypical molecules used in the study of the NLO properties of molecular systems. Therefore, it has been used frequently as a threshold value for comparative purposes. The calculated values of polarizability are 45.4385 x 10^{-24}, 46.7769 x 10^{-24}, 48.5591 x 10^{-24} and 24.2384 x 10^{-24} esu respectively; the values of anisotropy of the polarizability are 6.7340, 6.9323, 7.1965 and 3.5921 esu, respectively. The magnitude of the molecular hyperpolarizability (β_0) is one of the important key factors in a NLO system. The DFT/6-31G (d,p) calculated first hyperpolarizability value (β_0) of aryl sulfonyl piperazine derivatives are equal to 140.3301 x 10^{-33}, 171.1710 x 10^{-33}, 181.3870 x 10^{-33} and 62.9596 x 10^{-33} esu. The first hyperpolarizability of title molecules is approximately 0.41, 0.50, 0.53 and 0.18 times than those of urea (β of urea is 343.272 x10^{-33} esu obtained by B3LYP/6-311G (d,p) method). The above results show that all studied compounds **1-4** might have not the NLO applications.

4. CONCLUSION

Theoretical studies of the aryl sulfonyl piperazine derivatives **1-4** have been performed on the DFT calculations and B3LYP/6-31G (d,p) basis set. The molecular structural parameters of studied molecules have been computed in this work by using the same method cited above. The MEP map shows the negative potential sites are on sulfamide function as well as the positive potential sites around the hydrogen atoms. HOMO and LUMO energy gaps justify the eventual charge transfer interactions taking place within the molecule. The LUMO and HOMO energy provides information regarding ionization potential, chemical potential and other chemical descriptors and the results obtained shows that compound **3** is the most reactive. Mulliken charge analysis also supports the conjugation effect. The calculated Mulliken charges taking part in intramolecular charge transfer is also revealed in the natural bond orbital analysis. The stability of the molecule arising from hyper conjugative interactions, charge delocalization has been analyzed using NBO analysis which confirm charge transfer (π→π) arises within the molecule. The first hyperpolarizability is very smaller that of the standard NLO material urea and the aryl sulfonyl piperazine derivatives **1-4** molecules are not an attractive object for future studies of nonlinear optical properties.

Acknowledgments

This work was generously supported by the (General Directorate for Scientific Research and Technological Development, DGRS-DT) and Algerian Ministry of Scientific Research.

REFERENCES

1. Domagk G, Eine neue Klasse von Desinfektionsmitteln, Dtsch med Wochenschr, 1935; 61(21): 829-832. http://dx.doi.org/10.1055/s-0028-1129654.
2. Drew J, Drug discovery: a historical perspective, Science, 2000; 287:1960-1964.
3. Owa T, Nagasu T, Novel sulphonamide derivatives for the treatment of cancer, Exp Opin Ther Patents 2000; 10(11):1725-1740. https://doi.org/10.1517/13543776.10.11.1725.
4. Supuran CT, Scozzafava A, Carbonic anhydrase inhibitors and their therapeutic potential. Exp. Opin. Ther. Patents, 2000; 10(5):575-600. https://doi.org/10.1517/13543776.10.5.575.
5. Supuran CT, Scozzafava A, Carbonic Anhydrase Inhibitors Curr Med Chem-Imm., Endoc. Metab. Agents, 2001; 1(1):61-97. https://doi.org/10.2174/1568013013359131.
6. Maren TH, Relations Between Structure and Biological Activity of Sulfonamides. Annu Rev Pharmacol Toxicol, 1976; 16:309-327. https://doi.org/10.1146/annurev.pa.16.040176.001521.
7. Boyd AE, Sulfonylurea Receptors, Ion Channels, and Fruit Flies, Diabetes, 1988; 37(7):847-850. https://doi.org/10.2337/diab.37.7.847.

8. Thornber CW, Isosterism and molecular modification in drug design, Chem. Soc. Rev, 1979; 8(4):563-580. Available: https://doi.org/10.1039/CS9790800563.
9. Ogden RC, Flexner CW, Protease Inhibitors in AIDS Therapy, New York, U.S.A: Marcel Dekker; 2001.
10. Supuran CT, Scozzafava A, Mastrolorenzo A, Bacterial proteases: current therapeutic use and future prospects for the development of new antibiotics, Exp. Opin. Therap. Patents, 2001; 11(2):221-259. https://doi.org/10.1517/13543776.11.2.221.
11. Scozzafava A, Supuran CT, Carbonic Anhydrase and Matrix Metalloproteinase Inhibitors: Sulfonylated Amino Acid Hydroxamates with MMP Inhibitory Properties Act as Efficient Inhibitors of CA Isozymes I, II, and IV, and N-Hydroxysulfonamides Inhibit Both These Zinc Enzymes, J. Med. Chem, 2000; 43(20):3677-3687. https://doi.org/10.1021/jm000027t.
12. Parr RG, Yang W, Density Functional Theory of Atoms and Molecules, Oxford University Press, New York, 1989.
13. Srivastava AK, Pandey AK, Jain S, Misra N, FT-IR spectroscopy, intra-molecular C–H···O interactions, HOMO, LUMO, MESP analysis and biological activity of two natural products, triclisine and rufescine: DFT and QTAIM approaches, Spectrochim. Acta A, 2015; 136:682-689. https://doi.org/10.1016/j.saa.2014.09.082.
14. Narendra Sharath Chandra JN, Sadashiva CT, Kavitha CV, Rangappa KS, Synthesis and in vitro antimicrobial studies of medicinally important novel N-alkyl and N-sulfonyl derivatives of 1-[bis(4-fluorophenyl)-methyl]piperazine, Bioorg. Med. Chem, 2006; 14(19):6621-6627. https://doi.org/10.1016/j.bmc.2006.05.064.
15. Dennington R, Keith T, Millam J, Gaussview, Version 5, Semichem. Inc.,Shawnee Missions, KS, 2009.
16. Frisch MJ, Trucks GW, Schlegel HB, Scuseria GE, Robb MA, Cheeseman JR, et al, Gaussian 09, Revision C.01; Gaussian Inc.: Wallingford, CT, USA, 2010.
17. Becke AD. Density-functional thermochemistry. III. The role of exact exchange, J. Chem. Phys, 1998; 1998(7): 5648-5652. https://doi.org/10.1063/1.464913.
18. Gunasekaran S, Balaji RA, Kumeresan S, Anand G, Srinivasan S. Can, Experimental and theoretical investigations of spectroscopic properties of N-acetyl-5-methoxytryptamine, J. Anal. Sci. Spectrosc, 2008; 53:149-160.
19. Kavitha E, Sundaraganesan N, Sebastian S, Molecular structure, vibrational spectroscopic and HOMO, LUMO studies of 4-nitroaniline by density functional method, Ind. J. Pure Appl. Phys. 2010; 48:20-30.
20. Geerlings P, Proft FD, Langenaeker W, Conceptual Density Functional Theory, Chem. Rev. 2003; 103(5):1793-1873. https://doi.org/10.1021/cr990029p.
21. Jug K, Maksic ZB, in: Z.B. Maksic (Ed.), Theoretical Model of Chemical Bonding, Part 3, Springer, Berlin, 1991, p. 233.
22. Xiao-Hong L, et al, Calculation of vibrational spectroscopic and NMR parameters of 2-Dicyanovinyl-5-(4-N,N-dimethylaminophenyl) thiophene by ab initio HF and density functional methods, Comput. Theor. Chem, 2011; 969(1-3):27-34. https://doi.org/10.1016/j.comptc.2011.05.010.
23. Bailey RT, Dines TJ, Tedford MC, Electron-phonon coupling in the molecular charge transfer crystal 2-(α-methylbenzylamino)-5-nitropyridine, J. Mol. Struct, 2011; 992(1-3):52-58. https://doi.org/10.1016/j.molstruc.2011.02.035.